EARTH SURFACE PROCESSES AND LANDFORMS
Earth Surf. Process. Landforms **34**, 1245–1254 (2009)

Published online 24 April 2009 in Wiley InterScience
(www.interscience.wiley.com) DOI: 10.1002/esp.1809

The effects of interdune vegetation changes on eolian dune field evolution: a numerical-modeling case study at Jockey's Ridge, North Carolina, USA

Jon D. Pelletier,[1]* Helena Mitasova,[2] Russell S. Harmon[2] and Margery Overton[3]
[1] Department of Geosciences, University of Arizona, Tucson, Arizona, USA
[2] Department of Marine, Earth, and Atmospheric Sciences, North Carolina State University, Raleigh, North Carolina, USA
[3] Department of Civil, Construction, and Environmental Engineering, North Carolina State University, Raleigh, North Carolina, USA

Received 9 September 2008; Revised 22 January 2009; Accepted 9 February 2009

* Correspondence to: Jon D. Pelletier, Department of Geosciences, University of Arizona, 1040 East Fourth Street, Tucson, AZ 85721, USA.
E-mail: jdpellet@email.arizona.edu

ESPL
Earth Surface Processes and Landforms

ABSTRACT: Changes in vegetation cover within dune fields can play a major role in how dune fields evolve. To better understand the linkage between dune field evolution and interdune vegetation changes, we modified Werner's (*Geology*, 23, 1995: 1107–1110) dune field evolution model to account for the stabilizing effects of vegetation. Model results indicate that changes in the density of interdune vegetation strongly influence subsequent trends in the height and area of eolian dunes. We applied the model to interpreting the recent evolution of Jockey's Ridge, North Carolina, where repeat LiDAR surveys and historical aerial photographs and maps provide an unusually detailed record of recent dune field evolution. In the absence of interdune vegetation, the model predicts that dunes at Jockey's Ridge evolve towards taller, more closely-spaced, barchanoid dunes, with smaller dunes generally migrating faster than larger dunes. Conversely, the establishment of interdune vegetation causes dunes to evolve towards shorter, more widely-spaced, parabolic forms. These results provide a basis for understanding the increase in dune height at Jockey's Ridge during the early part of the twentieth century, when interdune vegetation was sparse, followed by the decrease in dune height and establishment of parabolic forms from 1953-present when interdune vegetation density increased. These results provide a conceptual model that may be applicable at other sites with increasing interdune vegetation cover, and they illustrate the power of using numerical modeling to model decadal variations in eolian dune field evolution. We also describe model results designed to test the relative efficacy of alternative strategies for mitigating dune migration and deflation. Installing sand-trapping fences and/or promoting vegetation growth on the stoss sides of dunes are found to be the most effective strategies for limiting dune advance, but these strategies must be weighed against the desire of many park visitors to maintain the natural state of the dunes. Copyright © 2009 John Wiley & Sons, Ltd.

KEYWORDS: eolian dunes; numerical modeling; biogeomorphology

Introduction

The evolution of many eolian dunes is strongly controlled by vegetation. Vegetation increases the aerodynamic roughness length of the surface, stabilizing the vegetation-covered portions of dunes (Sarre, 1989; Lancaster and Baas, 1998; Hugenholtz *et al.*, 2008). Conceptual models linking dune-field activity to climate change tend to treat dune fields as either wholly 'active' or 'inactive' depending on the threshold vegetation density (e.g. Hugenholtz and Wolfe, 2005). In detail, however, the evolution of partially-vegetated dune fields depends critically on the spatial distribution of vegetation within the dune field. Baas and Nield (2007), for example, explored the co-evolution of dune morphology and vegetation for partially-vegetated dunes using a numerical model. In this model, vegetation growth is favored on the trailing arms of incipient dunes where the magnitude of erosion and deposition falls within a certain range conductive to vegetation growth. Vegetation growth, in turn, limits erosion and deposition on trailing arms. In this way, vegetation cover, rates of erosion and deposition, and dune morphology co-evolve under certain conditions to create parabolic dunes that migrate at a steady rate. Duran and Herrmann (2006) also developed a model that couples eolian transport and erosion/deposition with the growth and death of plants. Their model was capable of quantifying the transition from active to inactive dunes as a function of vegetation density.

The response of active dune fields to changes in vegetation density through time is less well understood, however. In the US, the Outer Banks of North Carolina has been a particularly

well studied area, but many questions remain. Dune mobilization due to loss of vegetation in the Outer Banks during the nineteenth century resulted in development of rapidly moving, destructive barchan dunes or médanos in many areas (Cobb, 1906). Some of these dunes were artificially stabilized, e.g. to construct the Wright Brothers Memorial. Unfortunately, the limited quality of early aerial photographs (1932 and 1949) does not allow clear identification of the barchans mentioned in the literature, although some can be inferred from aerial photographs acquired in 1949 (Mitasova *et al.*, 2005). After construction of protective dunes in the 1930s (Birkemeier *et al.*, 1984), interdune vegetation in the Outer Banks increased from sparse to dense over the following 50 years. Outside of the US, dune stabilization due to vegetation 'invasion' has been reported at other locations such as the Tottori sand dunes in Japan (Onishi, 2006) as well as dunes near Cresmina, Portugal (Rebelo *et al.*, 2002). The goal of this paper is to better understand the cause-and-effect relationship between the density of interdune vegetation and dune field evolution.

Jockey's Ridge, North Carolina is the largest active dune complex on the east coast of the US and provides a suitable test case for our investigation. The recent evolution of this dune field is unusually well constrained following the work of Mitasova *et al.* (2005). These authors used airborne LiDAR surveys to map the dune field evolution at high spatial resolution (1·8 m/pixel) in 1999 and 2001. Historical aerial photographs and topographic maps enabled changes in dune height and vegetation cover to be constrained over the past century. Changes in dune area were quantified from 1974 to 2001. Jockey's Ridge is comprised of four major dunes, labeled (clockwise from left in Figure 1) west, main, east, and south dunes. Recent long-term net sand transport at Jockey's Ridge is approximately due south (Havholm *et al.*, 2004), leading to predominantly south-directed dune migration at relatively steady rates of 3–6 m/yr. While the net sand-transport direction is to the south, southerly (i.e. north-directed) winds do occur, resulting in slipface reversals and episodic north-directed dune migration for short periods of time. Also, despite the southward net transport direction, the slip faces of the major dunes have migrated in complex ways (i.e. the white arrows in Figure 1), reflecting the possible impact of hurricanes with strong, rotating wind fields.

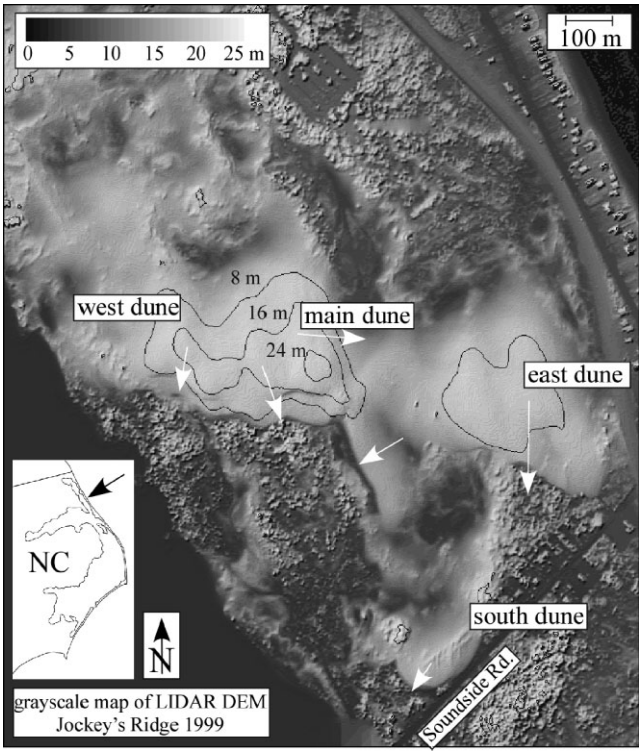

Figure 1. Grayscale map of elevations at Jockey's Ridge, North Carolina, in 1999, as determined from an airborne LiDAR survey. White arrows indicate direction and relative magnitude of recent (1974–2001) dune migration.

Mitasova *et al.* (2005) inferred a rapid increase in height of the main dune between 1915 and 1953 from approximately 20 to 40 m, followed by gradual decrease back to nearly 20 m from 1953 to the present. The recent dune deflation was accompanied by decrease in windward slope of the main dune from 5° to 2·5° between 1974 and 2005 and an increase in the area of the dune field by approximately 15% during that time period. Figure 2 illustrates the change in dune field morphology from 1974 to 1999. The results of recent surveys, up to and including 2008, show a continuation of this trend of decreasing dune height. Figure 2(A) illustrates the digital elevation model (DEM) of Jockey's Ridge in 1974, as constructed from historical topographic contour maps. The color map of change between 1974 (Figure 2A) and 1999 (Figure 1) illustrated in Figure 2(B) indicates the predominantly southward migration of dunes and the loss of peak elevation between 1974 and 1999. The transition from increasing to decreasing height of the main dune in the early 1950s coincided with an increase in interdune vegetation density documented in historical aerial photographs (Mitasova *et al.*, 2005). The establishment of dense interdune vegetation has been attributed to the construction of a linear foredune along the Outer Banks beaches in the 1930s (Birkemeier *et al.*, 1984). However, Havholm *et al.* (2004) argued that climate change is a major driver of dune evolution at Jockey's Ridge. The geological surveys conducted by Havholm *et al.* (2004) discovered two layers of soil within the dune indicating that the area changed from active dune to forest twice over the past 1000 years.

Dune migration has posed a persistent threat to the infrastructure in the vicinity of Jockey's Ridge in recent years, particularly along Soundside Road (Figure 1). In response, park managers have used sand redistribution and fencing to mitigate the southward migration and deflation of the dune field. Sand fencing installed at the south dune has slowed dune migration and triggered growth in the height of this dune but it did not stop the dune from exiting the park (Mitasova *et al.*, 2005). Approximately 125 000 m^3 of sand was removed from the south dune and deposited along the northern edge of the park in the winter of 2003. Both of these techniques have been somewhat effective in limiting the amount of sand exiting the park, but questions remain as to how to manage the larger dunes to preserve the natural landforms while minimizing the export of sand from the park. For example, where should sand be relocated and where should fences be installed in order for these strategies to be the most effective? Are there other mitigation strategies that could be more useful? In this paper, we use numerical modeling to test the efficacy of alternative mitigation strategies in order to provide guidance to land managers at Jockey's Ridge and in similar areas where rapidly-migrating dunes threaten infrastructure. More broadly, our goal in this paper is to use numerical modeling to explore the relationships between dune evolution and the spatial distribution of vegetation using Jockey's Ridge as a type of example. The purpose of the modeling is not to reproduce the exact details of the recent evolution of Jockey's Ridge, but instead to gain a better conceptual and quantitative understanding of how dune fields respond to changes in the spatial distribution of vegetation and management intervention.

DOI: 10.1002/esp

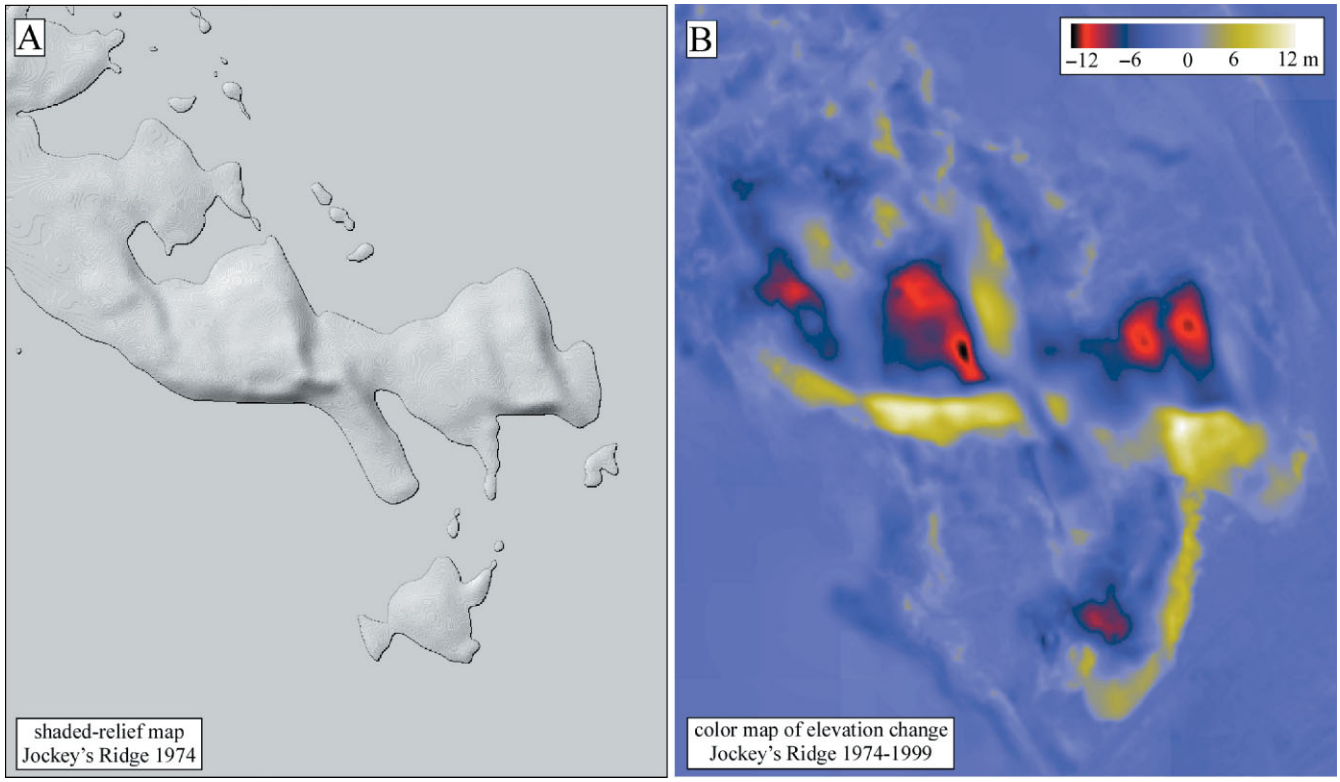

Figure 2. Maps illustrating change in Jockey's Ridge dune field from 1974 to 1999. (A) Grayscale map of Jockey's Ridge elevations in 1974 as determined from historical contour maps (Mitasova *et al.*, 2005). (B) Color map of change in elevations from 1974 to 1999. Areas of denudation appear in black and red, while areas of aggradation appear as yellow and white. This figure is available in colour online at www.interscience.wiley.com/journal/espl

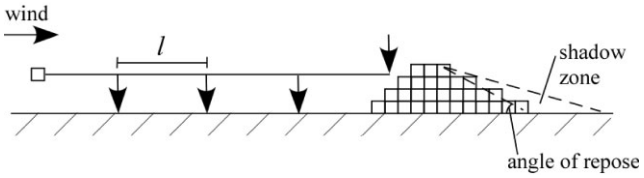

Figure 3. Schematic diagram of Werner's (1995) model of eolian dune evolution.

Model Description

The model we developed is a modified version of the dune field evolution model of Werner (1995). Werner (1995) was the first to model the formation of eolian dunes numerically from an initially flat surface. Werner's (1995) model (Figure 3) is based on the iterative entrainment, transport, and deposition of discrete units of sand that are picked up at random, transported a characteristic distance l downwind, and deposited back onto the surface with a probability p_s that is, by default, equal to 0·5. Sand units that are not deposited after the first 'jump' of distance l are transported repeatedly downwind until deposition occurs. In this way, the local sand flux depends on the values of l and p_s input into the model. In Werner's model, the effect of air flow over incipient dunes is included in a simplified way by defining 'shadow' zones where the probability of deposition is one. Shadow zones are defined to be areas located in shadow when the surface is illuminated by a sun angle of 15° from the horizontal and parallel to the wind direction. In Werner's model, shadow zones provide a simplified representation of the recirculation zone on the lee sides of incipient dunes where wind-driven sediment flux is low and deposition rates are high. Sand units deposited back down on the bed in Werner's model roll down the direction of steepest descent if deposition causes an oversteepened condition (i.e. a slope angle greater than the angle of repose). Werner's model combines three basic elements that, taken together, are responsible for the complex self-organized behavior observed in the model. First, the stochastic model of entrainment generates structureless, multi-scale relief from an initially flat bed. Second, shadow zones provide a mechanism for a positive feedback between the topography of incipient dunes and the spatial pattern of erosion and deposition that enhances dune height and spacing over time. Finally, avalanching provides a limitation on dune slope and a mechanism for cross-wind sand transport. Werner's model is capable of reproducing the four principal dune types (transverse, barchan, star, and linear) by varying sand supply and wind direction variability.

Werner's model forms the basis for a recent numerical model that explores the co-evolution between dunes and vegetation (Baas and Nields, 2007; Baas, 2007). In the Baas and Nields' model, empirical curves are used to relate vegetation growth and decay to the local rate of erosion and deposition. Vegetation density, in turn, influences the probability of deposition, p_s, in the model. In this paper, we take an alternative approach. First, we introduce a probability of entrainment, p_e, that varies according to the local vegetation density. Second, rather than modeling vegetation growth and decay explicitly through time, vegetation density and its effect on sediment flux is included using a prescribed relationship between the probability of entrainment, p_e, and elevation above that of the lowest interdune areas. In the Werner (1995) model, sand units are entrained from the surface with an equal probability at each pixel. In the model of this paper, the probability of entrainment, p_e, varies spatially depending on the local elevation, which is used as a proxy for vegetation density. In the model, a sand unit chosen at random from all the pixels in the model is

DOI: 10.1002/esp

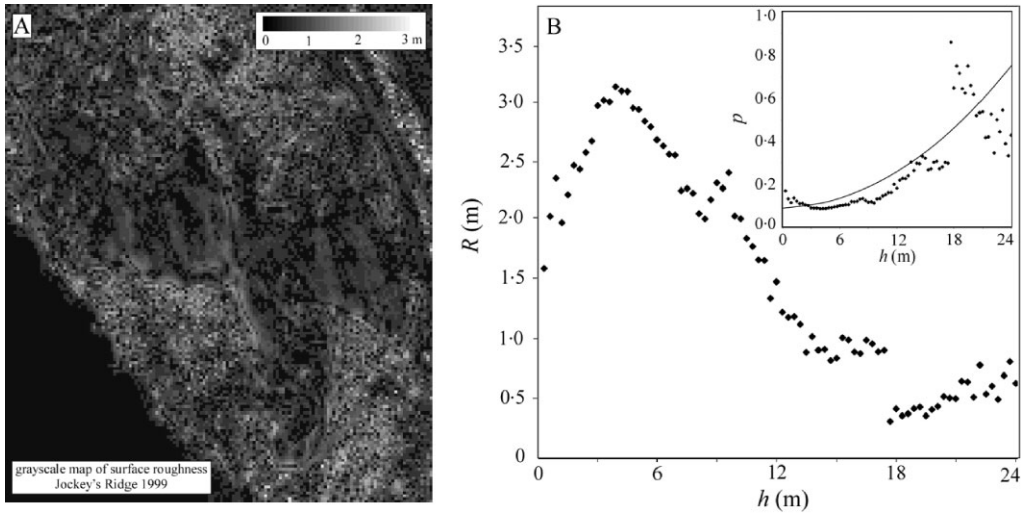

Figure 4. (A) Grayscale map of surface roughness of Jockey's Ridge in 1999, illustrating the relatively smooth dune surfaces in comparison to the rough interdune areas. (B) Plot of average surface roughness as a function of elevation. Areas of higher surface roughness (i.e. vegetation cover will have lower rates of particle entrainment. In the model, the probability of entrainment is assumed to be inversely proportional to roughness (inset). The solid curve in the inset graph illustrates the quadratic relationship between entrainment probability and elevation used in the model.

entrained if a random variable between zero and one is less than the local, elevation-dependent value of p_e, which also varies between zero and one. Otherwise, nothing happens during that time step. This elevation-dependent entrainment rule is calibrated specifically for the Jockey's Ridge site (calibration described later) using the relationship between surface roughness and elevation before and after the establishment of interdune vegetation beginning in the early 1950s. Prior to the early 1950s, the vegetation density at Jockey's Ridge was negligible (Mitasova *et al.*, 2005). As such, the original Werner (1995) model can be used to model dune evolution during this time period. After the early 1950s, the development of interdune vegetation stabilized low elevations but did not significantly affect sediment entrainment at higher elevations where vegetation density is negligible. For the post-1950s period, therefore, it is appropriate to vary p_e spatially according to elevation in order to represent the stabilizing effects of vegetation at low elevations.

In order to constrain the relationship between entrainment probability and elevation in the post-1950s era at Jockey's Ridge, consider Figure 4. Figure 4(A) illustrates a map of the surface roughness of Jockey's Ridge in 1999 computed from the 1·8 m/pixel resolution digital surface model (DSM) derived from the first return LiDAR data that include top of vegetation. This map represents the absolute value of the difference between the maximum and minimum elevations within a prescribed distance from each pixel, given here by 7·3 m or four pixels. In other words, Figure 4(A) plots the relief of the topography (including vegetation, man-made infrastructure, and all other roughness elements resolved in the DSM) at spatial scales of 7·3 m. In this paper we use the term surface roughness to describe the small-scale terrain relief measured in this way. This should not be confused with the aerodynamic roughness length. Figure 4(B) plots the relationship between the surface roughness mapped in Figure 4(A) and elevation above sea level, illustrating the inverse relationship between these two variables. In areas devoid of vegetation and other roughness elements, namely the areas with dunes that make up the high-elevation portions of the landscape, surface roughness values are typically between 0 and 1 m. Conversely, low-elevation zones (e.g. elevations between 0 and 6 m) are characterized by surface roughness values typically between 2 and 3 m.

Sediment flux is inversely correlated with the local surface roughness: areas of higher local-scale relief (e.g. taller and denser vegetation) will have correspondingly lower eolian sediment fluxes due to the sheltering effect of those roughness elements. The relationship between surface roughness and sediment flux is complex. In the model of this paper we assume a simple inverse proportionality between these two variables. The inset plot in Figure 4(B) plots the inverse of surface roughness as a function of elevation. The continuous solid curve in the inset graph is a parabolic fit to the data. This plot suggests that the probability of entrainment, p_e, can be modeled using a parabolic function of elevation, h, during the post-1950s era at Jockey's Ridge:

$$p_e \propto h^2. \tag{1}$$

More generally, one can assume that the relationship between p_e and h is a power-law relationship with exponent b: $p_e \propto h^b$. This power-law relationship is useful for understanding the transition between the different types of behavior exhibited by the model as the exponent b is varied continuously from zero (i.e. Werner's model) to two (Equation 1). In the model, the maximum probability is set to one for a reference elevation close to the highest elevation value in the model, i.e.

$$p_e = \left(\frac{h}{30\ \text{m}}\right)^2. \tag{2}$$

In Equation 2, the probability of entrainment is nearly zero for elevations close to zero and rises quadratically with elevation to a maximum value of one at an elevation of 30 m (i.e. close to the maximum elevation of the model at any time during the model runs presented in this paper).

In addition to the entrainment-elevation relationship represented by Equation 2, we also introduced an east–west gradient in entrainment probability into the model. The motivation for this model component is the mobility of the east dune, which in recent years has been (along with the south dune) the most active dune in the dune field. The east dune is the most susceptible to high bed shear stresses due to its proximity to the ocean. Dunes further inland experience lower shear stresses for the same far-field wind speeds due to the greater surface roughness (i.e. vegetation, infrastructure,

DOI: 10.1002/esp

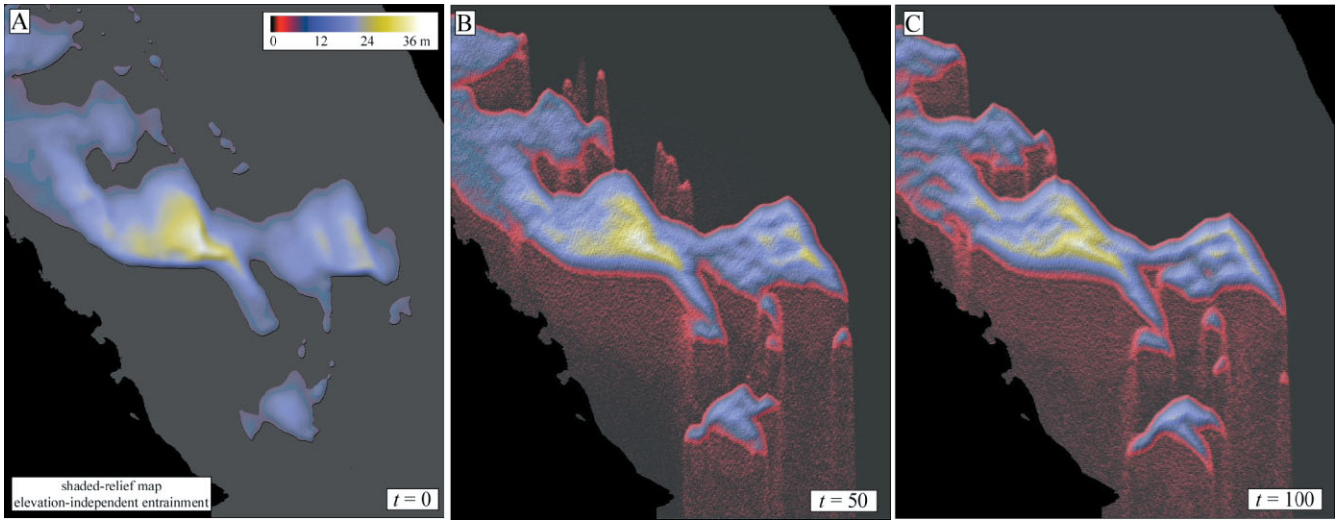

Figure 5. Color maps of dune evolution in the reference model with no vegetation (i.e. spatially uniform entrainment) for (A) $t = 0$ (Jockey's Ridge in 1974), (B) $t = 50$, (C) and $t = 100$. Units of time in the model are arbitrary but can be calibrated using measured and modeled dune migration rates. This figure is available in colour online at www.interscience.wiley.com/journal/espl

etc.) upwind from those dunes. In the model, we prescribed a higher entrainment probability on the east side of the study area using the relationship

$$p_e = \left(\frac{h}{30\ \text{m}}\right)^2 \left(\frac{x}{1200\ \text{m}}\right). \quad (3)$$

where x is the distance from the western boundary of the model. Equation 3 increases the entrainment probability from zero (along the western boundary of the model) to a maximum value close to one (along the eastern boundary of the model) as a linearly-increasing function of x.

Model Results

Figure 5 illustrates the results of the Werner (1995) model applied to Jockey's Ridge using the 1974 DEM of Jockey's Ridge constructed by Mitasova *et al.* (2005) as the initial condition for this model run. How the dune field evolves from this state provides insight into the potential trends in dune field evolution if all surrounding vegetation was removed and the initial dune was surrounded by a flat sheet of sand. In the model, areas that had no significant sand cover in 1974 were made equal to 0·3 m in the model. The model was run with input parameters $I = 9$ m (5 pixels) and $p_s = 0{\cdot}5$. The values of I and p_s influence the average rate of dune migration and the wavelength of instabilities produced by the model, but otherwise the values of I and p_s do not influence the trends in dune modification with or without interdune vegetation documented in this paper. Time in the model is arbitrary (and depends on the values of I and p_s), but the model can be calibrated to real time by comparing measured and modeled migration rates for a given study site over a given interval of time. The units of time are normalized to the number of grid points, so $t = 1$ refers to the time at which transport has been attempted, on average, once in each of the pixels in the model. No sand entered the model domain from the northern boundary but sand was allowed to leave from the bottom boundary. Sand that was transported into the ocean or sound from within the model domain was also removed from the system. Sand transport in the model takes place in a due south direction, reflecting the northerly winds that contribute the most to sand transport according to Havholm *et al.* (2004). The effects of variable substrate erodibility (e.g. soil horizons), changes in moisture (precipitation/evaporation) over time, and changes in the water table elevation over time were not considered in the model.

Over time, the model illustrated in Figure 5 develops more closely-spaced, barchanoid dunes that grow in height and decrease in total area, similar to those described for example by Cobb (1906). Over the example period illustrated in Figure 5, the main dune grows from 30 to 36 m and the total area of the dune field decreases from $4{\cdot}36 \times 10^5$ m^2 to $4{\cdot}21 \times 10^5$ m^2. The model also predicts that smaller dunes migrate somewhat faster than larger dunes (best illustrated in the change map of Figure 7A), but the east dune migrates the fastest due to the east–west gradient in flux imposed by Equation 3. The inverse correlation between dune height and migration rate in this model scenario (i.e. small dunes migrate faster than large dunes) is consistent with Bagnold's hypothesis that dune migration rate is inversely proportional to dune height assuming that sand transport rates are independent of dune height (Bagnold, 1941). Taller desert dunes are often observed to migrate at rates proportionately slower than shorter dunes because dune migration requires that the entire cross-section of the dune (which is proportional to height) be transported along the surface. Therefore, taller dunes will migrate more slowly than shorter dunes if sand transport rates are independent of dune height. The results illustrated in Figure 5 were obtained assuming no sand flux input from upwind of the study area. Introducing a constant influx of sediment along the upwind boundary has the effect of decreasing dune migration rates slightly, but the dune elevation does not change and the model results do not otherwise depend on the choice of boundary conditions.

Figure 6 illustrates the results of the model with elevation-dependent entrainment (i.e. Equation 3). Over time, this model develops paraboloidal dunes that decrease in height (the main dune decreases from 30 to 24 m) and increase in total area (from $4{\cdot}36 \times 10^5$ m^2 to $4{\cdot}51 \times 10^5$ m^2). Also, large dunes in this model migrate are rates comparable to that of smaller dunes (Figure 7B). This tendency can be understood as a result of the relationship between entrainment probability and elevation. In this model, sand transport rates over smaller dunes are lower than those over larger dunes because of the positive relationship between p_e and elevation. In the absence of this effect, small dunes migrate faster as described earlier. The lower sand transport rates of smaller dunes in this

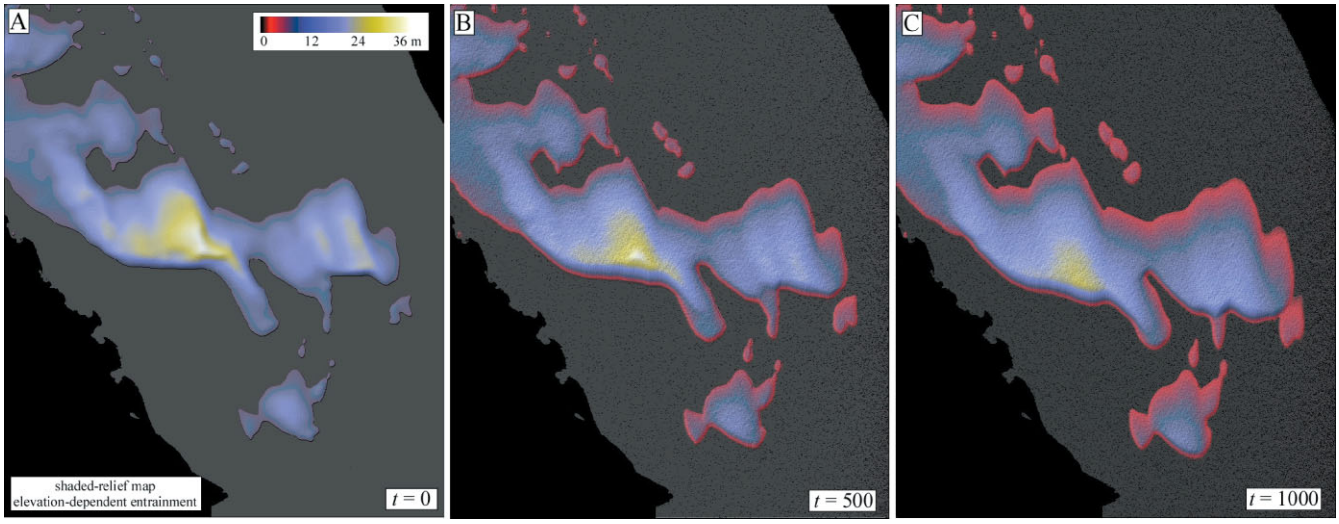

Figure 6. Color maps of dune evolution in the revised model with interdune vegetation (i.e. elevation-dependent entrainment) for (A) $t = 0$ (Jockey's Ridge in 1974), (B) $t = 500$, (C) and $t = 1000$. This figure is available in colour online at www.interscience.wiley.com/journal/espl

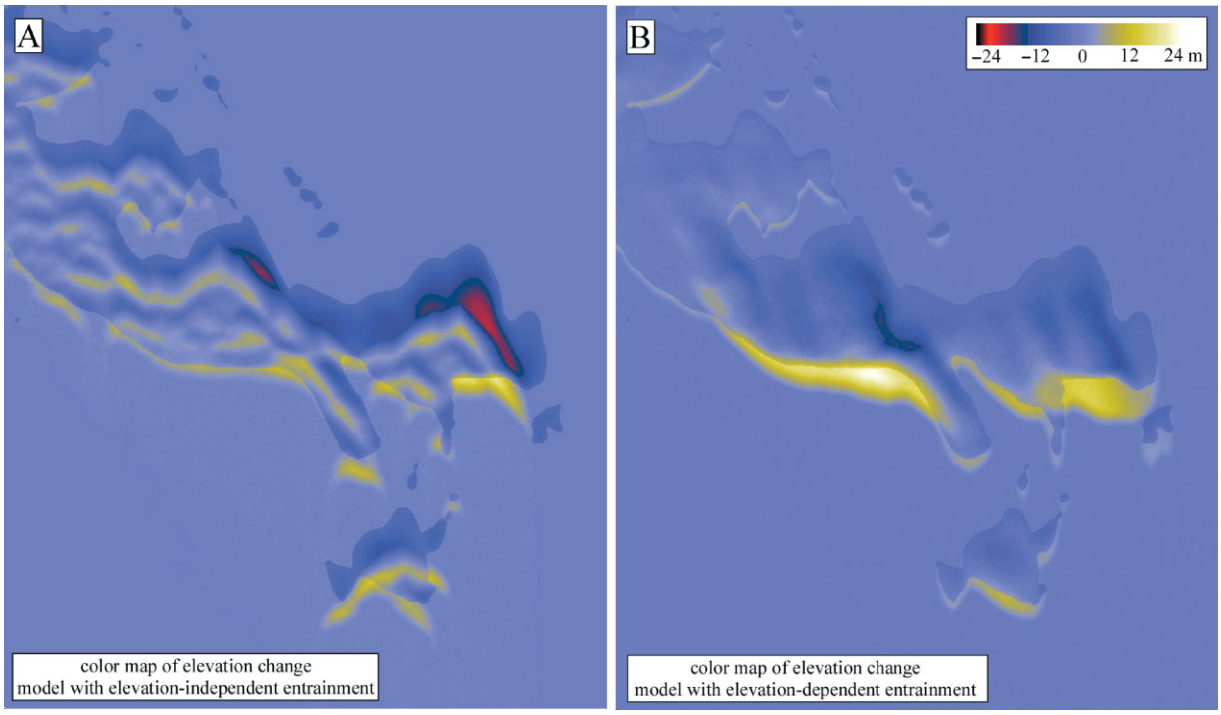

Figure 7. Color maps of elevation change between the beginning and end of the models illustrated in (A) Figure 5 and (B) Figure 6, highlighting the spatial distribution of erosion/deposition and dune migration. This figure is available in colour online at www.interscience.wiley.com/journal/espl

vegetation-controlled system offsets the geometric effect that causes large dunes to migrate more slowly in areas with sparse or no vegetation cover, thereby causing large dunes to migrate at rates similar to small dunes. Note that in Figure 5 (no vegetation), dune migration of approximately 100 m requires only a fraction of the time (i.e. $t = 100$ versus $t = 1000$) required in the model of Figure 6. The lower average rate of dune migration in Figure 6 reflects the stabilizing effects of vegetation (i.e. the overall lower probability of entrainment) in this model relative to that of Figure 5.

Figures 5 and 6 suggest that dune field evolution in the presence of interdune vegetation cover can be characterized by two alternative states. In the absence of interdune vegetation, dune fields develop taller, barchanoid-shaped dunes with small dunes migrating faster than larger dunes (although the east–west gradient in transport adds additional complexity to the relationship between dune size and migration rate in this case). In the presence of interdune vegetation, dune fields evolve towards shorter, paraboloidal dunes with large dunes migrating at rates comparable to those of smaller dunes. The transition between these two end-member states can be investigated within the model framework by using the power-law relationship between p_e and h (i.e. $p_e \propto h^b$) with different values of b. Model results with this generalized entrainment-elevation relationship (not shown) illustrate that the transition between these two end-member states occurs at $b = 1$. Dunes grow in height and develop barchanoid dunes for all values of b less than one and decrease in height and develop paraboloidal dunes for all values of b greater than one. Therefore, the essential criterion for determining dune morphology and evolution is not the presence or absence of interdune vegetation, but rather the functional form of the relationship between vegetation

DOI: 10.1002/esp

density and elevation. If sediment flux decreases rapidly with elevation (if, for example, a 50% increase in elevation results in a 90% decrease in sediment flux), then the system will be in the $b > 1$, deflating-dune regime. In contrast, if sediment flux decreases more slowly with increasing elevation (e.g. a 50% increase in elevation results in a 30% decrease in sediment flux), then the system will be in the $b < 1$, growing-dune regime.

Approximately 125 000 m^3 of sand was removed from the leading (southern) edge of the Jockey's Ridge dune field and deposited at its northern edge in the year 2003. This redistribution of sand, in and of itself, is a useful strategy for protecting the nearby infrastructure from dune encroachment. Indeed, given the volume and migration rate of the dune field, it is possible to estimate the mean annual volume of sand that must be redistributed in order to balance the action of the wind. Given the current dune-field volume of approximately 3×10^6 m^3 (Mitasova *et al.*, 2005), a migration rate of 5 m/yr, and a transported distance of 1000 m, and northerly prevailing winds, it would be necessary to relocate approximately 15 000 m^3 of sand each year in order to achieve a long-term balance between anthropogenic transport to the north and natural eolian transport to the south. Ideally, however, the sand would be relocated in such a way as to minimize the subsequent dune migration and encourage the development of taller dunes.

Figure 8 illustrates the results of numerical experiments aimed at quantifying the effect of sand redistribution on subsequent dune advancement and growth/deflation. We modeled the anthropogenic transport of sand by removing 6 m of sand from all pixels where the slope angle exceeded 20º (i.e. dune slip faces, labeled as 'sources' in Figure 8A). This hypothetical source distribution is not meant to represent the actual redistribution of sand that has occurred at Jockey's Ridge. In fact, redistributed sand has been sourced from the south dune only. Nevertheless, slip faces provide one possible source region for sand redistribution generally, as slip faces are the leading edge of dunes and hence the sand that most immediately threatens infrastructure. Removing a fixed thickness of sand from all slip faces and redistributing that sand upwind represents one possible strategy for mitigating dune field advance. Sand removed from slip faces in the model was deposited north of the crestline of the main dune complex by a fixed 'relocation distance' (360 m in the example of Figure 8A). Figure 8B plots the subsequent relative migration rates of the dune field as a whole as a function of the relocation distance. Sand that was relocated onto the dune crestline (i.e. equal to a 'relocation distance' of zero from the crestline) had the greatest impact on subsequent migration rates in the model, causing a decrease of approximately 6·5%. Sand that was relocated at progressively greater distances from the crestline had a correspondingly lower effect on subsequent migration rates. Sand redistribution had no significant effect on dune height: maximum dune height with and without sand redistribution and for different distances of sand redistribution differed by less than 0·5 m in simulations of the dune-field evolution following sand redistribution. Over all, these results indicate that sand redistribution has only a marginal effect on subsequent dune migration and growth. However, the effect of sand redistribution can be maximized by relocating the sand as close as possible to the crestline.

The installation of sand-trapping fences has also been used at the south dune of Jockey's Ridge. Repeat LiDAR surveys indicate that these fences have slowed the rate of migration and promoted an increase in the height of this dune (Mitasova *et al.*, 2005). In the model, the effect of sand-trapping fences was simulated by lowering the probability of entrainment to zero within a prescribed 'trapping' distance upwind and downwind from each fence. Sand can still be transported past the fence, but only by depositing sand until the angle of repose is achieved and subsequent transport occurs by avalanching. Figure 9(A) illustrates the dune field evolution following the installation of three fences placed 9 m apart along the crestline of the main dune complex with a trapping distance of 1·8 m for each fence. Figure 9(B) illustrates that the migration rate following fence installation decreased by 12%. Fences located upwind and downwind of the crestline had a progressively smaller effect on subsequent migration rates in the model. The magnitude of the relative decrease in migration rates depends on the number, spacing, and height (i.e. trapping distance) of the fences. Therefore, the 12% reduction in migration rates is only illustrative. The maximum height of the main dune height increases in these cases, but this effect is associated primarily with the buildup of sand in the immediate vicinity of the fences. The results in Figure 9(B) illustrate that fence installation has a greater effect on subsequent dune

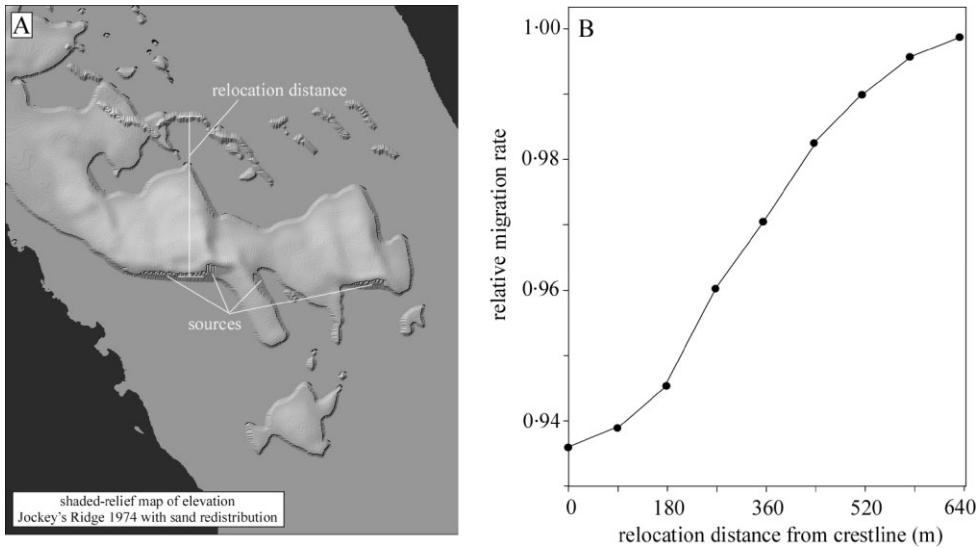

Figure 8. Illustration of the effect of sand redistribution on subsequent dune migration rates. (A) Shaded-relief map of elevations input into the model immediately following sand redistribution at $t = 0$. Sand was removed from slip faces and transported by a characteristic relocation distance upwind from the peak. (B) Plot of the relative migration rate following sand redistribution as a function of the relocation distance, illustrating that the greatest reduction in migrations rates occurs for sand redistributed to the crestline.

DOI: 10.1002/esp

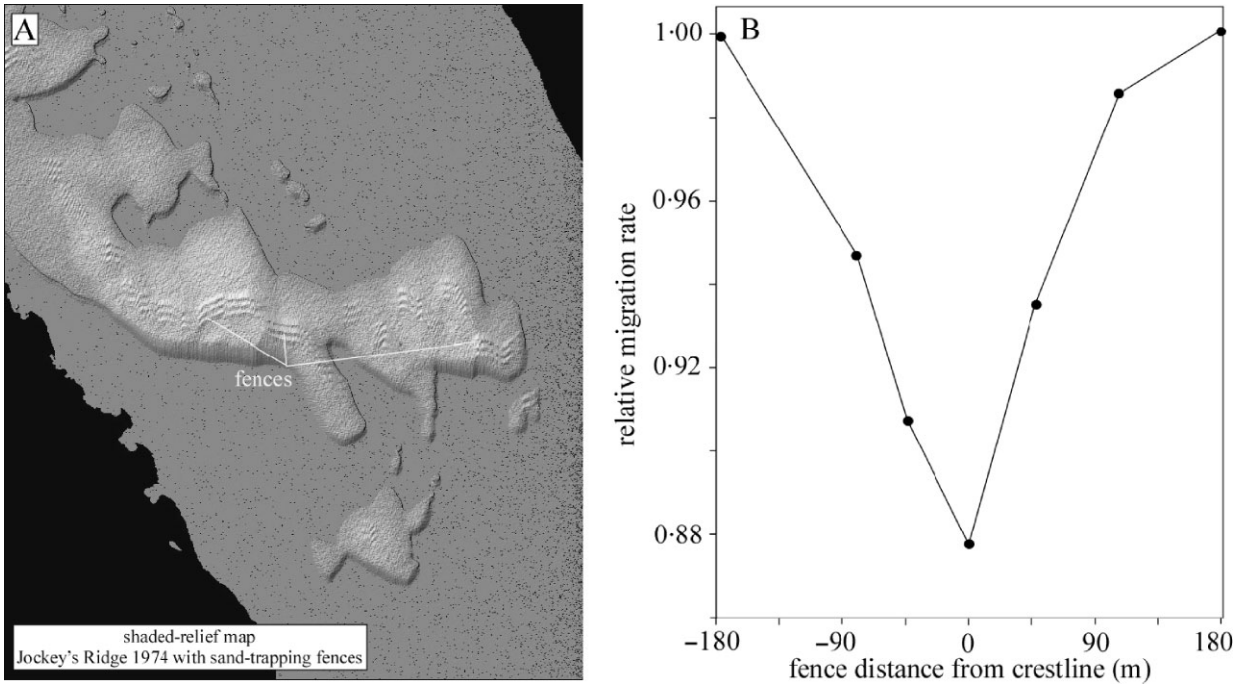

Figure 9. Illustration of the effect of fence installation on subsequent dune migration rates. (A) Shaded-relief map of elevations input into the model immediately following fence installation at $t = 0$ for the case with fences placed along the dune crestline. (B) Plot of the relative migration rate following fence installation as a function of the distance from the peak, illustrating that the optimal fence location is along the dune crestline.

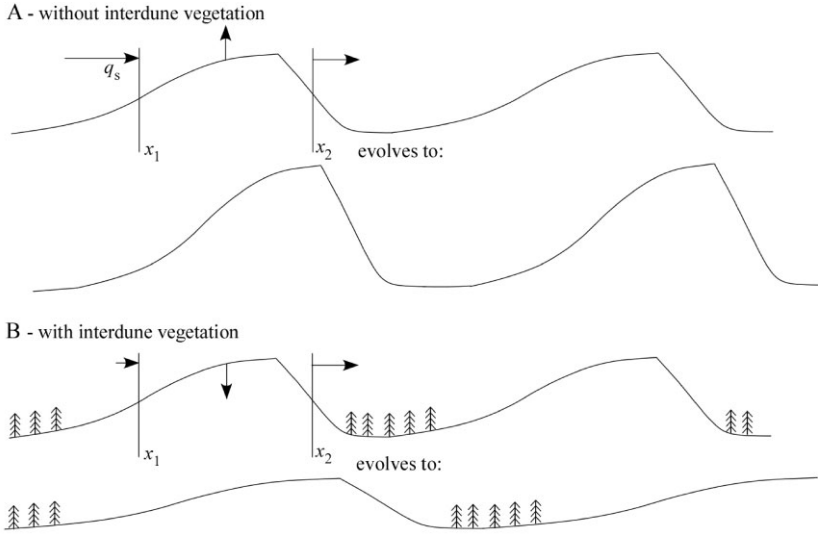

Figure 10. Schematic diagram of the conceptual model for the effect of interdune vegetation on dune evolution.

migration compared to the sand redistribution mitigation strategy.

Discussion

The relationship between dune growth/deflation and interdune vegetation illustrated in Figures 5 and 6 can be best understood using a conceptual model based on mass conservation principles. Consider Figure 10, which illustrates this conceptual model as it applies to dunes with and without interdune vegetation. In Figure 10(A), a dune segment is identified with upwind and downwind cross-sections located at x_1 and x_2, respectively. Conservation of mass applied to that segment implies that any difference in the volumetric sediment flux entering the section from upwind and leaving the section downwind must be accompanied by a change in the average elevation of the segment. Mathematically, conservation of mass along the sediment flux direction is quantified by Exner's equation, which states:

$$\frac{\Delta h}{\Delta t} = \frac{q_s(x_1) - q_s(x_2)}{x_2 - x_1} \tag{4}$$

where h is the average elevation of the segment between and x_1 and x_2 and q_s denotes the sediment flux. Equation 4 simply states that if the flux of sand is greater coming into the segment than the flux of sand leaving the segment, that difference must be stored within the segment, thereby causing aggradation. Conversely, if the flux of sand is greater leaving the segment than entering it, that difference must be supplied from sand within the segment, thereby causing surface lowering or denudation. In Figure 10(A), which represents the case with little or no interdune vegetation, the sediment flux

DOI: 10.1002/esp

entering the top portion of the dune will be greater than the sand leaving the lee side of the dune by avalanching. In this case, conservation of mass implies that the dune must grow in height. Figure 10(B) illustrates the alternative end-member scenario with relatively dense interdune vegetation. In this case, sediment flux entering the top of the dune will be relatively low due to the stabilizing effect of interdune vegetation upwind. As a result, more sand will leave the dune downwind than will enter the dune from upwind. The result in this case is dune deflation. Conservation of mass also implies that as dunes grow in height they must decrease in area, assuming that the dune field remains constant in volume. Conversely, deflating dunes will spread out and increase in area. The decrease in dune height and increase in dune area predicted by this model is consistent with the recent dune evolution at Jockey's Ridge from 1974 to present documented by Mitasova *et al.* (2005).

Earlier studies concluded that dune deflation at Jockey's Ridge was the result of nearby source depletion. Runyan and Dolan (2001) argued that the original source for the Jockey's Ridge sand probably came from a 'deflation' area immediate northeast of the dune field. This hypothesis implies that conditions favorable to dune growth (i.e. a plentiful supply of sand from the northeast) was disrupted by land management practices beginning in the 1930s, especially the construction of a protective barrier dune along the shore, and further increased with urban development in the 1960s, resulting in significantly lower sand supply. The model results of this paper, however, in addition to the conceptual model illustrated in Figure 10, suggest that dune growth and deflation is primarily the result of the redistribution of sand between dunes and interdune areas. Indeed, from 1974 to the present, Mitasova *et al.* (2005) documented that the maximum dune height decreased by 40% (from approximately 35 to 25 m) and that dune area increased by 15% (from 4·5 to $5{\cdot}3 \times 10^5$ m^2), while the change in total volume of the dune field was less than 10%. If dune deflation were a direct result of lower sand supply, it is reasonable to expect that dune height and volume would change in similar proportions. The fact that dune height decreases in far greater proportion than the dune-field volume implies that deflation is not primarily a result of a diminishing sand supply. Rather, dune deflation is primarily the result of sand redistribution within the dune field from dunes to interdune areas.

The mass conservation framework illustrated in Figure 10 has additional implications for land management strategies. This framework implies that increased dune height can be promoted by any change that increases the difference between the rate of sand flux entering and leaving the top sections of dunes. For example, the installation of fences or vegetation at or near the dune crestline serves to lower the flux of sand leaving the dune while having relatively limited impact on the rate of sand entering the dune from upwind. The mass conservation framework implies that stabilizing the topmost portions of dunes using vegetation or sand-trapping fences is perhaps the single most effective strategy for promoting taller dunes and limiting dune advancement. However, this strategy has a negative impact on the dunes as natural landforms and is more suitable for lower sections of the dunes to prevent their migration outside the park. Sand redistribution, in contrast, has little lasting effect on the spatial distribution of sediment fluxes, and hence has a lesser effect on subsequent dune growth and migration rates. Taller dunes could also be formed by devegetating interdune areas, but this measure would likely increase the overall rate of dune migration because of the uniformly higher rates of transport in a landscape with no vegetation cover. Dune-field devegetation has been carried out in the Netherlands as a management strategy, with the goal of enabling natural vegetative succession to occur in order to maximize species diversity, and, perhaps, minimize long-term dune migration. In such cases, sand 'drifts' analogous to the growing dunes in Figures 5(B) and 5(C) have developed over the short term, resulting in landscape destabilization and rapid dune migration in previously stabilized dune-field areas (van der Hagen *et al.*, 2008).

The Outer Banks of North Carolina are subject to intense hurricanes, and future research to quantify the impact of hurricanes specifically is needed. Hurricanes in this area generate both more intense winds and a shift from northerly to southerly winds. The effects of hurricanes are not captured by the LiDAR data of Mitasova *et al.* (2005) precisely, because immediate before and after surveys are not available, but data suggests that hurricanes flatten the dunes. The geomorphic effectiveness of these events is limited due to the significant rainfall that occurs during hurricanes. Northerly winds without rainfall have a much more significant impact (Havholm *et al.*, 2004). Mitasova *et al.* (2005) identified all major hurricanes and attempted to identify changes in evolution pattern or morphology. They found little evidence of major long-term impact, however; dunes generally flatten after hurricanes but rebuild relatively soon thereafter.

The model of this paper is limited and several caveats should be noted. First, a steady single wind direction was used representing winds that, on average, showed the most impact due to their frequency and intensity (Havholm *et al.*, 2004). In reality, the prevailing winds from March through August are from the southwest [9·9–12·8 miles per hour (m.p.h.)] while those from September through February are slightly stronger and from the northeast (10·8–13·4 m.p.h). There are anecdotal observations of dunes shifting back and forth in north–south direction as a result of this change in wind direction. Nevertheless, the long-term data presented by Mitasova *et al.* (2005) as well as the unpublished 2007 and 2008 data show steady southerly migration. Seasonal data would be needed to confirm quantitatively the impact of changing wind direction. Single storm effects can be simulated by using the wind direction and intensity for the modeled storm as well as adjusting the entrainment probability function to the state of vegetation during the storm (depending on seasons and previous weather patterns). Second, the relationship between surface roughness and elevation (Figure 4) represents an average for the study area. Some areas of low elevation within the dune field, however, have lower vegetation density than others. In these areas of lower-than-average vegetation density the model will underpredict the rate of dune activity downwind because the model is based on a study-area-wide average vegetation-elevation relationship. It should be noted that interdune areas within the Jockey's Ridge dune field are also ephemerally influenced by ponded water (Mitasova *et al.*, 2005). Ponds can trap sand during wet periods and later act as local sources of sand during dry periods. The limitations of the model are most apparent when comparing the observed evolution of the south dune from 1974 to 1999. This dune evolved from a dome-shaped dune to a classic parabolic dune over this period. The model with elevation-dependent entrainment reproduces the basic parabolic character of this dune but does not reproduce the detailed shape or relative migration rate. Additional model complexity, including spatially-explicit vegetation growth/decay and a variable sand transport rate and direction (e.g. to represent the episodic nature of transport during hurricanes), would be needed to refine the model behavior and better understand the short-term evolution of this dune field.

Despite these caveats, the methods used in this paper may help to unravel the complex forcing mechanisms of recent

DOI: 10.1002/esp

dune field evolution in both coastal and inland dune systems. There is abundant evidence for the role of vegetation changes in controlling the evolution of dune fields on the Israeli coast (Tsoar and Blumberg, 2002), southern Africa (Bullard *et al.*, 1997), and in Canada (Hugenholtz *et al.*, 2008), for example. In particular, the dunes studied by Tsoar and Blumberg (2002) have undergone a change from predominantly barchan and transverse dunes to parabolic dunes during a shift from relatively low to high vegetation density in the latter half of the twentieth century that closely mirrors the evolution at Jockey's Ridge. One key difference, however, between the Israeli and Jockey's Ridge cases is that the switch from barchan to parabolic dunes in the Israeli case was due to an increase in vegetation on the crests while at Jockey's Ridge it was due to an increase in interdune vegetation. In the Israeli case, vegetation growth on the crest led to an increase in the peak dune elevation, consistent with the conceptual model illustrated in Figure 10. Further work is needed to identify the range of conditions under which dunes may shift from barchan to parabolic types and from growing to deflating dunes.

For applications of the model to other dune fields, the relationship between surface roughness and elevation (Equation 2) must be derived based on the local data although the general assumption that roughness decreases with elevation is likely to be applicable to many other dune fields. Soil moisture reduces sand transport and supports vegetation growth, and its effect could be incorporated into the model as a control on entrainment using a similar function as Equation 2. However, soil moisture data are more temporally variable and harder to derive from remote sensing or on-ground measurements than vegetation cover. The model could also be used to simulate scenarios of increased drought and desertification as well as impact of increased rainfall sea level rise (increased wetness) leading to increased vegetation and dune stabilization by modification of the entrainment probability function.

Conclusions

Numerical modeling of dune evolution has advanced greatly in the past decade, primarily in response to the development of Werner's (1995) model. Here we modified Werner's model to account for the stabilizing effect of vegetation in dune fields in which there is a systematic relationship between vegetation density and elevation. We applied this model to the dune field at Jockey's Ridge, North Carolina, in order to better understand the trends in dune field evolution with and without interdune vegetation. The model illustrates the strong control that interdune vegetation can exert on dune field morphology and evolution. In the absence of interdune vegetation, dunes evolve towards closely-spaced, barchanoid dunes that increase in height and decrease in area through time, with smaller dunes migrating faster than larger dunes. The presence of interdune vegetation causes dunes to evolve towards more widely-spaced, parabolic dunes that decrease in height and increase in area through time, with small and large dunes migrating at roughly comparable rates. The recent evolution of dunes at Jockey's Ridge can best be understood within a mass-conservative framework that links local fluxes to vegetation density and the rate of change of surface elevation to the spatial variation in those fluxes. Finally, numerical modeling of alternative mitigation strategies underlines the effectiveness of introducing roughness elements (i.e. vegetation or fences) near the dune crestline; however, this strategy conflicts with the mission of the state park to conserve its natural features and is thus limited to the borders of the park. Although the model has been developed using the data from the Jockey's Ridge state park the model can be applied to coastal dunes evolving under similar conditions in different regions of the world. Modifications in the equation for entrainment probability function can be used to simulate impacts of increased subsurface water levels, sea water level rise or extended drought and change in vegetation.

Acknowledgements—The authors wish to thank reviewers Chris Hugenholtz and Karen Havholm for helpful reviews that greatly improved the paper. We also wish to thank chief editor Stuart Lane and the associate editor for additional helpful suggestions.

References

Baas ACW. 2007. Complex systems in aeolian geomorphology. *Geomorphology* **91**: 311–331.

Baas ACW, Nield JM. 2007. Modeling vegetated dune landscapes. *Geophysical Research Letters* **34**: L06405. DOI: 10.1029/2006GL029152

Bagnold RA. 1941. *The Physics of Blown Sand and Desert Dunes*. Methuen: London.

Birkemeier W, Dolan R, Fisher N. 1984. The evolution of a barrier island: 1930–1980. *Shore and Beach* **52**: 2–12.

Bullard JE, Thomas DSG, Livingstone I, Wiggs GFS. 1997. Dunefield activity and interactions with climatic variability in the southwest Kalahari Desert. *Earth Surface Processes and Landforms* **22**: 165–174.

Cobb C. 1906. Where the wind does the work. *National Geographic Magazine* **17**: 310–317.

Duran O, Herrmann HJ. 2006. Vegetation against dune mobility. *Physical Review Letters* **97**: L188001. DOI: 10.1103/PhysRevLett.97.188001

Havholm KG, Ames DV, Whittecar GR, Wenell BA, Riggs SR, Jol HM, Berger GW, Holmes MA. 2004. Stratigraphy of back-barrier coastal dunes, northern North Carolina and southern Virgina. *Journal of Coastal Research* **20**: 980–999.

Hugenholtz CH, Wolfe SA. 2005. Biogeomorphic model of dunefield activation and stabilization on the northern Great Plains. *Geomorphology* **70**: 53–70.

Hugenholtz CH, Wolfe SA, Moorman BJ. 2008. Effects of sand supply on the morphodynamics and stratigraphy of active parabolic dunes, Bigstick Sand Hills, southwestern Saskatchewan. *Canadian Journal of Earth Sciences* **45**: 321–335.

Lancaster N, Baas ACW. 1998. Influence of vegetation cover on sand transport by wind: field studies at Owens Lake, California. *Earth Surface Processes and Landforms* **23**: 69–82.

Mitasova H, Overton M, Harmon RS. 2005. Geospatial analysis of a coastal sand dune field evolution: Jockey's Ridge, North Carolina. *Geomorphology* **72**: 204–221.

Onishi N. 2006. In the shrinking dunes, stalking a creepy green enemy. *The New York Times*, 23 August. http://travel2nytimes.com/2006/08/23/world/asia/23japan.html [accessed 1 October 2008].

Rebelo LP, Brito PO, Monteiro JH. 2002. Monitoring the Cresmina dune evolution (Portugal) using differential GPS. *Journal of Coastal Research* **SI36**: 591–604.

Runyan KB, Dolan R. 2001. Origin of Jockey's Ridge, North Carolina: the end of the highest sand dune on the Atlantic Coast? *Shore and Beach* **69**: 29–32.

Sarre R. 1989. The morphological significance of vegetation and relief on coastal foredune processes. *Zeitschrift fur Geomorphologie Supplementband* **73**: 17–31.

Tsoar H, Blumberg DG. 2002. Formation of parabolic dunes from barchan and transverse dunes along Israel's Mediterranean coast. *Earth Surface Processes and Landforms* **27**: 1147–1161.

Van der Hagen HGJM, Geelen LHWT, de Vries CN. 2008. Dune slack restoration in Dutch mainland coastal dunes. *Journal for Nature Conservation* **16**: 1–11.

Werner BT. 1995. Eolian dunes: computer simulations and attractor interpretation. *Geology* **23**: 1107–1110.

Wilson IG. 1972. Aeolian bedforms: their development and origins. *Sedimentology* **19**: 173–210.